Identification of geraldol as an inhibitor of aquaporin-4 binding by NMO-IgG

JIE WANG[1], SHUAI WANG[2], MEIYAN SUN[3], HUIJING XU[3], WEI LIU[3], DELI WANG[2], LEI ZHANG[3], YAN LI[3], JIAMING CAO[2], FANG LI[2] and MIAO LI[4]

[1]Department of Neurology, The Third Hospital of Jilin University, Changchun, Jilin 130033; [2]School of Life Sciences, Jilin University, Changchun, Jilin 130012; [3]Medical Examination College, Jilin Medical University, Jilin, Jilin 132013; [4]Department of Neurosurgery, The Third Hospital of Jilin University, Changchun, Jilin 130033, P.R. China

Received August 22, 2018; Accepted August 27, 2019

DOI: 10.3892/mmr.2020.11212

Abstract. Neuromyelitis optica (NMO) is a severe neurological demyelinating autoimmune disease that affects the optic nerves and spinal cord. There is currently no effective cure or therapy. Aquaporin-4 (AQP4) is a known target of the autoimmune antibody NMO-IgG. Therefore, binding of NMO-IgG to AQP4, and subsequent activation of antibody-mediated and complement-dependent cytotoxicity (CDC), are thought to underlie the pathogenesis of NMO. In the present study, a cell-based high-throughput screening approach was developed to identify molecular inhibitors of NMO-IgG binding to AQP4. Using this approach, extracts from the herb *Petroselinum crispum* were shown to have inhibitory effects on NMO-IgG binding to AQP4, and the natural compound geraldol was purified from the herb extracts. Analytical high performance liquid chromatography, electrospray ionization-mass spectrometry and nuclear magnetic resonance analyses confirmed the identity of the isolated compound as geraldol, a flavonoid. Geraldol effectively blocked binding of NMO-IgG to AQP4 in immunofluorescence assays and decreased CDC in NMO-IgG/complement-treated FRTL-AQP4 cells and primary astrocytes. Geraldol exhibited low cytotoxicity, with no effect on proliferation or apoptosis of FRTL-AQP4 cells and primary astrocytes. Permeability assays indicated that geraldol did not alter the water transport function of AQP4 in either cell system. The present study suggests the potential therapeutic value of geraldol for NMO drug development.

Correspondence to: Dr Miao Li, Department of Neurosurgery, The Third Hospital of Jilin University, 126 Xiantai Street, Changchun, Jilin 130033, P.R. China
E-mail: limiao@jlu.edu.cn

Key words: neuromyelitis optica, autoimmune disease, aquaporin-4, neuromyelitis optica-IgG, geraldol

Introduction

Neuromyelitis optica (NMO), also known as Devic's syndrome, is a severe demyelinating disease of the central nervous system that causes recurrent seizures. NMO mainly affects the optic nerves and the spinal cord, but it can also affect the brain, to a lesser extent (1). NMO is difficult to distinguish clinically from multiple sclerosis (MS) as both disorders have similar characteristics in the early stages of disease. NMO was once considered a subtype of MS, and was even termed optica-spinal MS in Japan. However, a previous study has suggested that NMO is an independent clinical entity that is distinct from MS (2). NMO is caused by an autoimmune antibody (NMO-IgG) targeting aquaporin-4 (AQP4), a plasma membrane water transport channel expressed in the glia (3-5). Binding of NMO-IgG to AQP4 on astrocytes can cause complement-mediated and cell-mediated injury to astrocytes, triggering a series of inflammatory cascades that result in the release of cytokines, activation of microglia and accumulation of leukocytes. Together, these responses result in neuronal injury and cause the clinical symptoms of NMO (6-8).

NMO remains to be an incurable disease. The goal of treating acute NMO events is to improve relapse symptoms and restore neurological functions, while the aim of long-term immunosuppression is to prevent further attacks (9-11). For long-term immunosuppression, patients usually receive either B cell-targeted therapies, such as intravenous rituximab or oral azathioprine, and/or prednisone (12-20). Other therapeutic options include mycophenolate mofetil (21), methotrexate (22) or mitoxantrone. Mitoxantrone can cause adverse effects, such as cardiotoxicity or leukemia, and is thus generally not considered for first-line treatment (11,23-28). A novel strategy for NMO treatment is blocking the binding of NMO-IgG to AQP4. Based on this strategy, a high-affinity, non-pathogenic monoclonal antibody (aquaporumab) was developed and exhibited positive effects in clinical trials (29). Aquaporumab can relieve NMO symptoms by competing with NMO-IgG to bind to AQP4 (29). However, monoclonal antibody drugs can also have disadvantages, for example, they may activate the complement system and cause pathological changes similar to those

observed in NMO, or they may induce the production of autoimmune antibodies, thus reducing their protective effects (10).

In this context, inhibitors that block binding between NMO-IgG and AQP4 may represent potential drug candidates for treating NMO. A previously established reporter cell-based high-throughput screening system identified a small molecule inhibitor (isotetrandrine, obtained from an extract of the herb *Mahonia japonica*) that can block binding between NMO-IgG and AQP4 in a dose-dependent manner (30). In the present study, the natural compounds from another herb (*Petroselinum crispum*) that exhibited similar inhibitory effects in the screening system were purified. Another compound from this herb, geraldol, inhibited binding of NMO-IgG to AQP4.

Materials and methods

Cells, animals and antibodies. Chinese hamster lung fibroblast cells V79 (American Type Culture Collection; cat. no. CCL-93) were cultured in DMEM medium (D7777; Sigma-Aldrich; Merck KGaA). Fischer rat thyroid epithelial cells FRTL which exogenously expresses M23-AQP4 were supplied by Liaoning Medical College and established from a plasmid transfection (30). FRTL were cultured in F-12-modified Coon's medium (Sigma-Aldrich; Merck KGaA). Both culture media were supplemented with 10% (v/v) FBS (Sigma-Aldrich; Merck KGaA) and 2 mM glutamine. Cells were cultured at 37˚C under a humidified atmosphere containing 5% CO_2.

In total, 30 female (age, 6-week-old; weight ~18 g) and 20 male (age, 8-week-old; weight ~23 g) $AQP4^{-/-}$ mice (Dalian Medical University) were used in the present study, as previously described (31). Mice were housed in a 20-26˚C specific pathogen-free animal facility on a 12 h light/dark cycle and 15 times per hour air exchange, with constant access to food and water. Mice were mated until birth, then neonatal mice were used for primary astrocytes isolation. Protocols for mouse experiments were approved by the Laboratory Animal Ethics Committee of School of Life Science, Jilin University (Changchun, China; approval no. 2017-nsfc049).

NMO-IgG was purified from the sera of patients with NMO and concentrated using a Melon Gel IgG Purification kit (Thermo Fisher Scientific, Inc.) and Amicon Ultra Centrifugal Filter Units (EMD Millipore) according to the manufacturer's protocol. NMO serum and control (non-NMO) serum were obtained from clinical patients whose sera were NMO-IgG positive or negative, respectively (32). This study was approved by Ethics Committee of The China-Japan Union Hospital, Jilin University (approval no. 2017022238). Written informed consent was obtained from all patients.

Primary screening procedures. The procedure for primary screening of various herb fractions inhibiting the binding of NMO-IgG to AQP4 was performed as previously described (30). Briefly, V79-AQP4 cells were plated in black-walled and clear-bottomed 96-well tissue culture plates (Costar; Corning, Inc.) and maintained in complete DMEM at 37˚C for ~48 h until they reached 90% confluence. Overall, 80 wells were used to test natural fractions or natural compounds which were isolated and maintained in the lab of the present study; the first row of each plate was used as a negative control (V79-AQP4, no test compound) and the last row of each plate was used as a positive control (V79-null, no test compound). Each well was washed three times with PBS, fixed with 4% paraformaldehyde (PFA) at room temperature for 10 min and blocked with 3% BSA (Merck KGaA) at room temperature for 30 min (100 μl/well). Test natural fractions were added to each well (0.5 μl 20 mM solution in DMSO) and incubated for 15 min at room temperature. After washing twice with PBS, NMO-IgG (0.2 μg/ml) and horseradish peroxidase (HRP)-labeled goat anti-human IgG secondary antibody (1:1,000, Santa Cruz Biotechnology, Inc.; cat. no. sc-2907) were added to each well and incubated at 37˚C for 1 h. After washing three times with PBS, enhanced chemiluminescent substrate (ECL-Plus; GE Healthcare) was added to measure HRP activity. Chemiluminescence was measured after 5 min using a plate reader (TECAN Infinite 200; Tecan Group Ltd.).

Isolation and identification of target natural compounds. P. crispum was purchased from a commercial herb supplier (Hongjian Herb Store). The isolation procedures were performed as previously described (33). The aerial parts of *P. crispum* were crushed and extracted using different solvents (petroleum, ethyl acetate, chloroform, n-butanol; all were 100%; purchased from Beijing Chemical Works) at room temperature to achieve maximum solubility for the target peak (bioactive fraction). The extracts (50 g) were further purified by high-speed countercurrent chromatography (HSCCC; TBE-300; Tauto Biotechnique Co., Ltd.), which was coupled with a UV detector (cat. no. TBD-23UV; Tauto Biotech Co., Ltd.) with the following settings; Rotation rate, 800 rpm; solvent, 70% methanol; flow rate, 10 ml/min; three multilayer-coiled polytetrafluoroethylene columns (internal diameter, 3.0 mm; total volume, 300 ml) connected in series at a temperature of 25˚C. Each peak fraction was manually collected and concentrated using a rotatory evaporator under reduced pressure, yielding 1-4 g concentrate for each fraction. After bioactivity screening, four continuous peak fractions derived from ethyl acetate extraction were selected to isolate single compound. Then, 20 μg of each concentrate was dissolved in acetonitrile for subsequent analytical reverse-phase high performance liquid chromatography (HPLC; Shimadzu LC-2010AHT; Shimadzu Corporation) with a UV detector. Geraldol obtained from Sigma-Aldrich (Merck KGaA) was used as an internal reference compound. A 4.6x25 mm C18 column (particle size, 5 μm; Beckman Ultrasphere ODS) was used for peak separation at 20˚C. The mobile phase consisted of 52% methanol and 48% water containing 2% acetic acid. The injection volume was 10 μl and the flow rate was 1.0 ml/min. The effluent was examined at 360 nm. Peak identification was performed using liquid chromatography/mass spectrometry and nuclear magnetic resonance (NMR). Mass spectrometry was performed using QuattroMicro (Waters) equipment with scans from 50 to 1,000 m/z. The positive electrospray ionization (ESI) mode was used, with N_2 as the curtain gas, nebulizer gas and collision gas (11, 9 and 7 psi as the optimal values). The ESI needle voltage was set to 4,500 V and the turbo-gas temperature was set at 425˚C. ^{1}H and ^{13}C NMR spectra were recorded using a Bruker Avance 500 spectrometer (Bruker Optics-Beijing) operating at 500 MHz for ^{1}H and 100 MHz for ^{13}C spectra.

Primary astrocyte cultures. Primary astrocytes were isolated from the cortices of 20 1-day-old wild-type and AQP4$^{-/-}$ mice as previously described (34). Briefly, the cerebral hemispheres of the mice were separated, and the meninges, hippocampus, basal ganglia and olfactory bulb were removed. Cortical tissue was then isolated using forceps under a microscope, and digested in 0.25% trypsin-EDTA in DMEM at 37˚C for 15 min. The digested cells were centrifuged at 300 x g for 10 min at room temperature, and cultured on a poly-L-ornithine hydrobromide-coated (P3655; Sigma-Aldrich; Merck KGaA) 96-well plate or glass coverslips in DMEM supplemented with 10% FBS (Sigma-Aldrich; Merck KGaA) at 37˚C under a humidified atmosphere containing 5% CO_2. The medium was changed every other day. To purify astrocytes, the culture plates were shaken in a rotator at 180 rpm overnight and then at 220 rpm for 4 h when confluency reached ~30%. To prevent proliferation of other cell types, cell mixtures were treated with 10 μM cytosine arabinoside for 48 h. The medium was replaced with DMEM containing 3% FBS and 0.15 mM dibutyryl cAMP to induce differentiation when confluency reached ~50%. Once astrocyte confluency had reached >90%, the complement-dependent cytotoxicity (CDC) assay was performed.

CDC assay. For the CDC assay, cells were incubated with *P. crispum* fractions, isolated geraldol or DMSO for 15 min, followed by treatment of NMO-IgG (2.5 μg/ml) and 5% human complement (Sigma-Aldrich; Merck KGaA) for 1 h at 37˚C. Control human serum collected from patients without NMO (1:200) was added as a negative control. CellTiter-Glo® Luminescent Cell Viability Assay (Promega Corporation) was used to measure cell viability and its decrease according to CDC. Briefly, after incubation at 37˚C for 48 h, 100 μl of CellTiter-Glo® reagent was added to each well and mixed by gentle vortexing, swirling or inverting to obtain a homogeneous solution. Luminescence was recorded after 5 min using a microplate reader (Fluostar Optima; BMG Lab Tech GmbH). All experiments were repeated twice with four replicates.

Immunofluorescence staining. V79 cells expressing M23-AQP4 were cultured on round glass coverslips in 24-well plate (Corning, Inc.) for 24 h. After washing three times with PBS, the cells were blocked with 3% BSA (Merck KGaA) at room temperature for 1 h. Geraldol or DMSO was added in 3% BSA and incubated at room temperature for 15 min, followed by the addition of NMO-IgG (20 μg/ml) or control serum from patients without NMO (1:200) at room temperature for 1 h. V79-AQP4 cells were washed with PBS three times and incubated with Alexa Fluor 555-conjugated goat anti-human IgG secondary antibody (1:400; Invitrogen; Thermo Fisher Scientific, Inc; cat. no. A-21433). For AQP4 immunofluorescence staining, V79-AQP4 cells were fixed in 4% PFA at room temperature for 10 min and permeabilized with 0.5% Triton X-100 at room temperature for 10 min. After blocking with 3% BSA at room temperature for 1 h, the cells were incubated with rabbit anti-AQP4 antibody (1:200; Santa Cruz Biotechnology; cat. no. sc-32739) at room temperature for 1 h. Alexa Fluor 488-conjugated goat anti-rabbit IgG (1:200; Invitrogen; Thermo Fisher Scientific, Inc.; cat. no. A32731) was used as the secondary antibody. Fluorescence images were obtained and observed using fluorescence microscopy (IX71; Olympus Corporation).

Cell viability assay. Cell viability was measured in 96-well plates with a colorimetric assay using the Cell Proliferation reagent (WST-1; Roche; cat. no. 11644807001) according to the manufacturer's protocol. Cells at 70% confluency were treated with serial dilutions of geraldol (2, 4, 8, 16, 32, 64, 128 or 256 μM) for 24 h. WST-1 reagent (10 μl/well) was added to cultured cells (100 μl/well) and incubated at 37˚C for 1 h. Absorbance was measured at 440 nm. All experiments were repeated twice with 4 replicates.

Detection of apoptosis. Apoptosis was detected using a Cell Death Detection ELISA^{PLUS} kit (Roche) according to the manufacturer's protocol. This photometric enzyme immunoassay is used for quantitative *in vitro* detection of cytoplasmic histone-associated DNA fragments (mono- and oligo-nucleosomes) following programmed cell death. Cells at 70% confluency were treated serial dilutions of geraldol (2, 4, 8, 16, 32, 64, 128 or 256 μM) for 24 h. Cell lysates were then placed in a streptavidin-coated microplate and incubated with a mixture of biotinylated anti-histone and anti-DNA peroxidase antibodies that were included in the kit at room temperature for 2 h. The amount of peroxidase retained in the immunocomplex was photometrically determined after reaction with 100 μl 2,2'-azinobis(3-ethylbenzothiazoline-6-sulfonic acid)-diammonium salt substrate at room temperature for 15 min. Absorbance was measured at 405 nm. All experiments were repeated twice with four replicates.

Osmotic water permeability assay. Osmotic water permeability of the plasma membrane was assessed using a slightly modified version of a previously described calcein fluorescence quenching method (31). Briefly, cells were cultured on glass coverslips pre-coated for 24 h, incubated with 5 μM calcein-AM (Invitrogen; Thermo Fisher Scientific, Inc.) at 37˚C for 15 min, and then transferred to a perfusion chamber designed for rapid solution exchange. The time course of cytoplasmic calcein fluorescence in response to cell shrinkage induced by exchange of perfusate between PBS (300 mOsmol) and hypertonic PBS (500 mOsmol containing 200 mM D-mannitol) was measured. A reciprocal exponential time constant (τ=1/s) was used as an indicator of cell shrinkage, where τ is the time from the initiation of the osmotic switch to the point where cytoplasmic calcein fluorescence quenching reaches its maximum. All experiments were repeated twice with four replicates.

Statistical analysis. Statistical analysis was performed using the unpaired two-tailed Student's t-test in SPSS (version 17.0; SPSS, Inc.). Multiple comparisons between groups were performed using a one-way ANOVA followed by Sidak multiple comparisons test with GraphPad Prism software (version 7; GraphPad Software, Inc.). Data are expressed as the mean ± standard deviation. $P<0.05$ was considered to indicate a statistically significant difference.

Results

Isolation and structural characterization of geraldol. Fractions from the herb *P. crispum* were isolated by solvent extraction and subject to a screening as reported in a previous

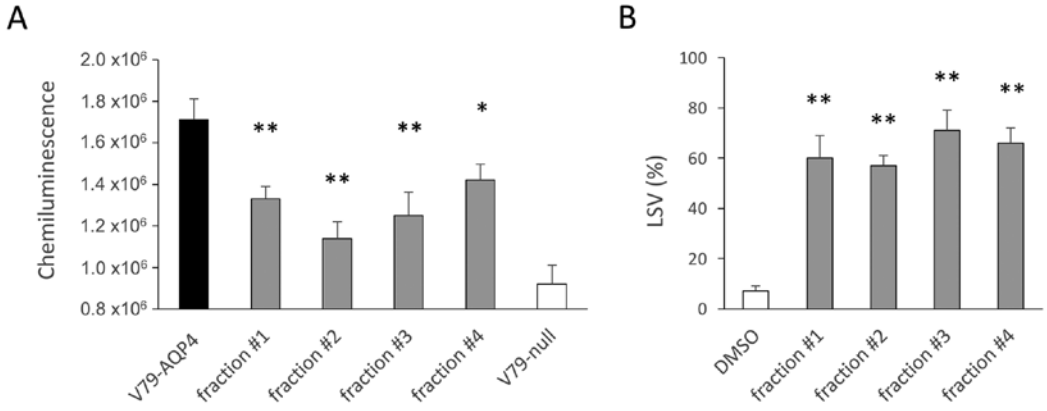

Figure 1. Inhibitory effects of four *Petroselinum crispum* fractions on the binding of NMO-IgG to AQP4 in primary and secondary screens. (A) Inhibitory effects on NMO-IgG binding to AQP4 in primary screens. *P<0.05; **P<0.01 vs. V79-AQP4 group. (B) Inhibitory effects on NMO-IgG-dependent complement cytotoxicity in secondary screens. LSV increase (%)=($LSV_{samples}$-$LSV_{V79\text{-}AQP4}$)/($LSV_{V79\text{-}null}$-$LSV_{V79\text{-}AQP4}$) x100. n=3. **P<0.01 vs. DMSO group. NMO, neuromyelitis optica; LSV, luminescence signal value; AQP4, aquaporin 4.

study (30). During the primary screening, four continuous fractions isolated from ethyl acetate extraction were identified to have inhibitory effects on NMO-IgG binding to AQP4 (Fig. 1A). These fractions also exhibited inhibitory effects on NMO-IgG-dependent complement cytotoxicity in secondary screens (Fig. 1B).

This bioactivity-guided phytochemical study led to the isolation of the flavonoid geraldol from all the four fractions. The purity of the compound was assessed using analytical HPLC. As presented in Fig. 2, only a single peak with a retention time of 47.74 min was observed. The purity of the peak was determined to be 99.5%. These results indicated that >99% pure geraldol could be obtained successfully using HSCCC separation under optimized conditions. The HSCCC-purified fraction was structurally characterized using ESI-mass spectrometry (ESI-MS) and NMR as follows:

Molecular formula: $C_{16}H_{12}O_6$. ^{1}H NMR (500 MHz, $CDCl_3$): δ (ppm) 7.93 (^{1}H, d, J=8.8 Hz, H-5), 6.91 (^{1}H, dd, J=2.2 Hz, 8.8 Hz, H-6), 6.97 (^{1}H, d, J=2.2 Hz, H-8), 7.77 (^{1}H, d, J=2.1 Hz, H-2'), 6.94 (^{1}H, d, J=8.5 Hz, H-5'), 7.70 (^{1}H, dd, J=2.1 Hz, 8.5 Hz, H-6'), 9.66 (^{1}H, s, OH-3), 10.74 (^{1}H, s, OH-7), 9.08 (^{1}H, s, OH-4') and 3.83 (^{1}H, s, OCH_3-3'). ^{13}C NMR (100 MHz, CD_3OD): δ (ppm) 144.9 (C-2), 137.3 (C-3), 172.0 (C-4), 126.4 (C-5), 114.7 (C-6), 162.3 (C-7), 102.1 (C-8), 156.3 (C-9), 114.2 (C-10), 122.6 (C-1'), 111.7 (C-2'), 147.4 (C-3'), 148.4 (C-4'), 115.5 (C-5'), 121.4 (C-6') and 55.6 (OCH_3-3').

Geraldol blocks NMO-IgG binding to AQP4. The inhibitory effect of geraldol on NMO-IgG binding to AQP4 was analyzed using immunofluorescence assays. After the V79-AQP4 cells were incubated with NMO-IgG, fixed and permeabilized, binding of Alexa Fluor 555-conjugated anti-human secondary antibody was measured in the presence or absence of geraldol. As presented in Fig. 3, red fluorescence was decreased when cells were incubated with geraldol. Meanwhile, an anti-C terminal AQP4 antibody and Alexa Fluor 488-labeled secondary antibody were used to test the expression of AQP4. The green fluorescence produced by staining with anti-C terminal AQP4 antibody was unaltered by geraldol treatment. There was an approximately equal total number of cells in the different groups (indicated by light microscopy).

Geraldol decreases CDC in both NMO-IgG/complement-treated FRTL-AQP4 cells and primary astrocytes. Next, the inhibitory effects of geraldol on CDC were evaluated. FRTL cells stably expressing human AQP4 were incubated with NMO-IgG for 60 min in the presence of human complement, along with either geraldol or DMSO. The cytotoxicity of geraldol was also measured using this system. As presented in Fig. 4A, geraldol increased the viability of NMO-IgG/complement-treated FRTL-AQP4 cells in a concentration-dependent manner. The half maximal inhibitory concentration (IC_{50}) of geraldol was 24.6 μM. A group of FRTL cells without AQP4 expression were used as the negative control. In order to confirm the effects of geraldol purified from a natural source, a commercial geraldol compound was also purchased and its inhibitory effects were tested in the same CDC assay with similar results (data not shown).

The inhibitory effect of geraldol on CDC was also assessed in cultured primary astrocytes from wild-type and $AQP4^{-/-}$ mice (Fig. 4B). Geraldol increased the viability of cultured NMO-IgG/complement-treated primary astrocytes from wild-type mice in a concentration-dependent manner. The IC_{50} of geraldol was 30.3 μM. No inhibitory effect was observed in cultured primary astrocytes from $AQP4^{-/-}$ mice.

Geraldol does not affect the viability of FRTL-AQP4 cells and primary astrocytes. To determine whether geraldol affects cell viability, its effects on cell proliferation were analyzed using the WST-1 assay and cell apoptosis using the cell death assay. As presented in Fig. 5A and B, no significant differences in cell proliferation or apoptosis were observed within the geraldol dose range used in the present study.

Geraldol does not affect the water permeability of FRTL-AQP4 cells and primary astrocytes. Whether geraldol influences the osmotic water permeability of AQP4 was further investigated in the present study. Using a calcein-AM fluorescence quenching-based method as previously described (31), geraldol did not significantly influence osmotic water permeability in either FRTL-AQP4 cells or astrocytes (Fig. 6).

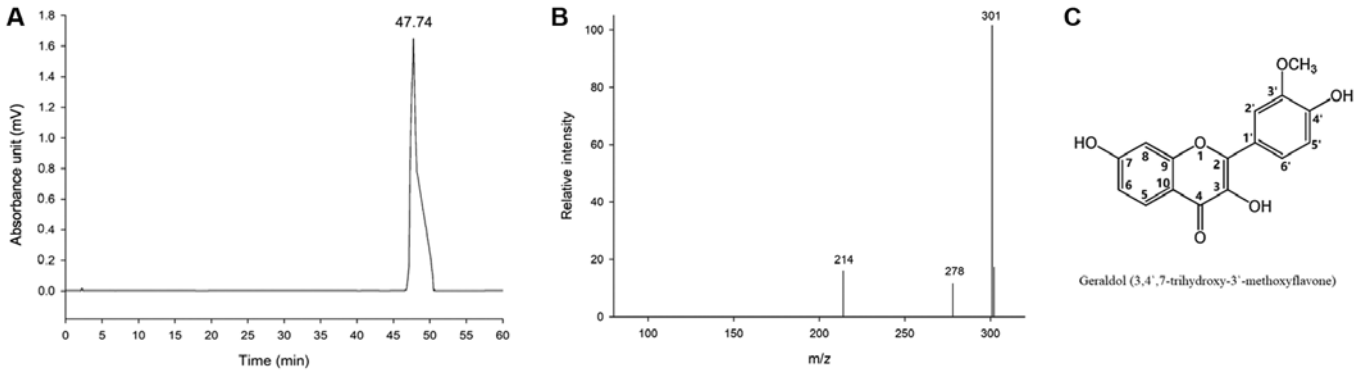

Figure 2. (A) Representative HPLC chromatogram, (B) mass spectrum and (C) and structure of the isolated compound, geraldol. Reverse-phase HPLC analysis was performed using the C18 Octadecyl-silica chromatographic column (5 μm, 4.6x200 mm) at a flow rate of 1.0 ml/min. HPLC, high performance liquid chromatography; AU, absorbance unit.

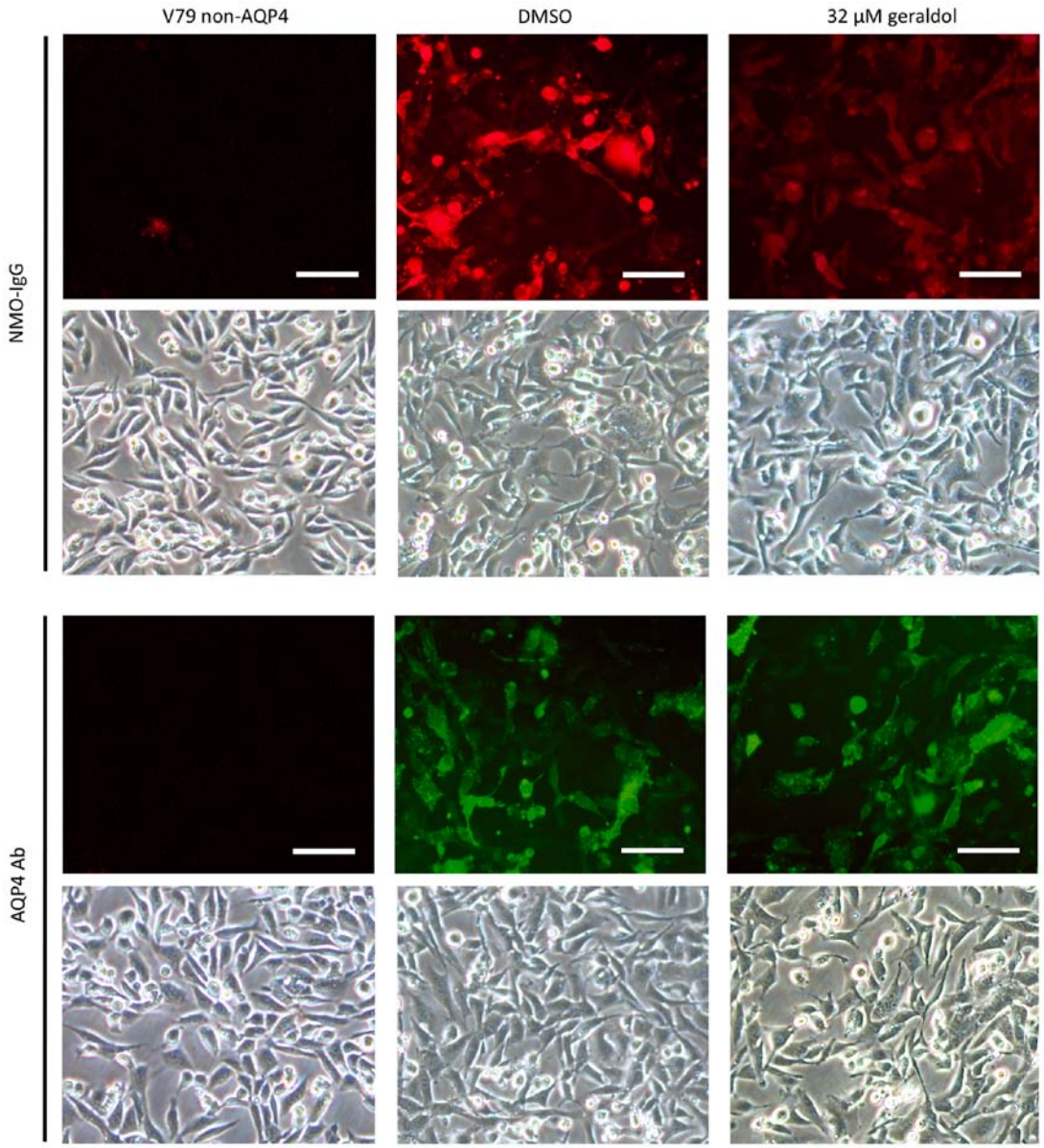

Figure 3. Immunofluorescence images exhibiting the effect of geraldol on NMO-IgG binding to AQP4. V79-AQP4 cells were incubated with 32 μM geraldol or DMSO prior to antibody addition. Non-AQP4-expressing V79 cells were used as a negative control. First row, staining with NMO-IgG and an Alexa Fluor 555-conjugated anti-human secondary antibody (red). Second and fourth row, there were, approximately, an equal total number of cells in the different groups. Third row, staining with rabbit anti-AQP4 antibody and an Alexa Fluor 488-conjugated anti-rabbit secondary antibody (green). Scale bar, 50 μm. AQP4, aquaporin 4; NMO, neuromyelitis optica; Ab, antibody.

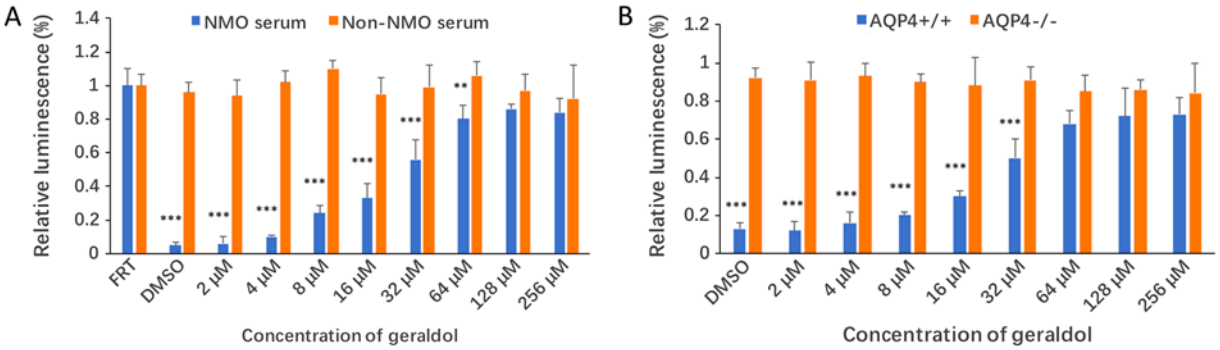

Figure 4. Effects of geraldol on CDC in NMO-IgG/complement-treated FRTL-AQP4 cells (A) and primary astrocytes (B). CDC was measured for cells exposed to either NMO-IgG or non-NMO patient serum and complement in the presence of the indicated concentrations of geraldol (n=4). **P<0.01, ***P<0.001 vs. respective AQP$^{-/-}$ group. CDC, complement-dependent cytotoxicity; NMO, neuromyelitis optica; AQP4, aquaporin 4.

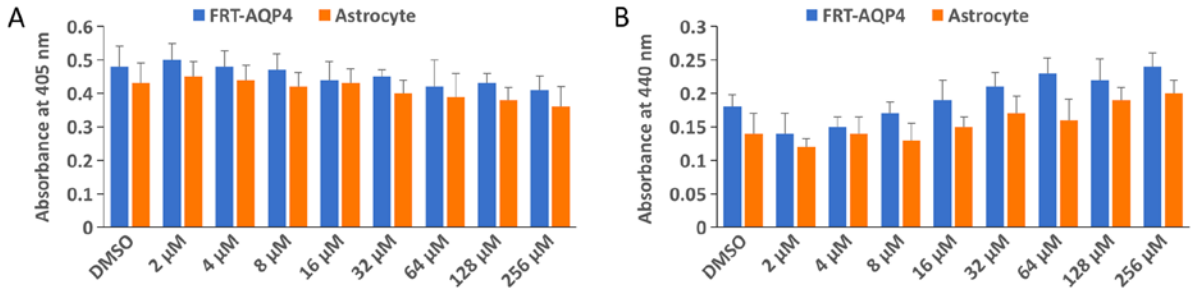

Figure 5. Effect of geraldol on proliferation and apoptosis of FRTL-AQP4 cells and primary astrocytes. (A) Cell proliferation in the presence of the indicated concentrations of geraldol measured using a WST-1 assay (n=4). (B) Cell death in the presence of the indicated concentrations of geraldol (n=4). AQP4, aquaporin 4.

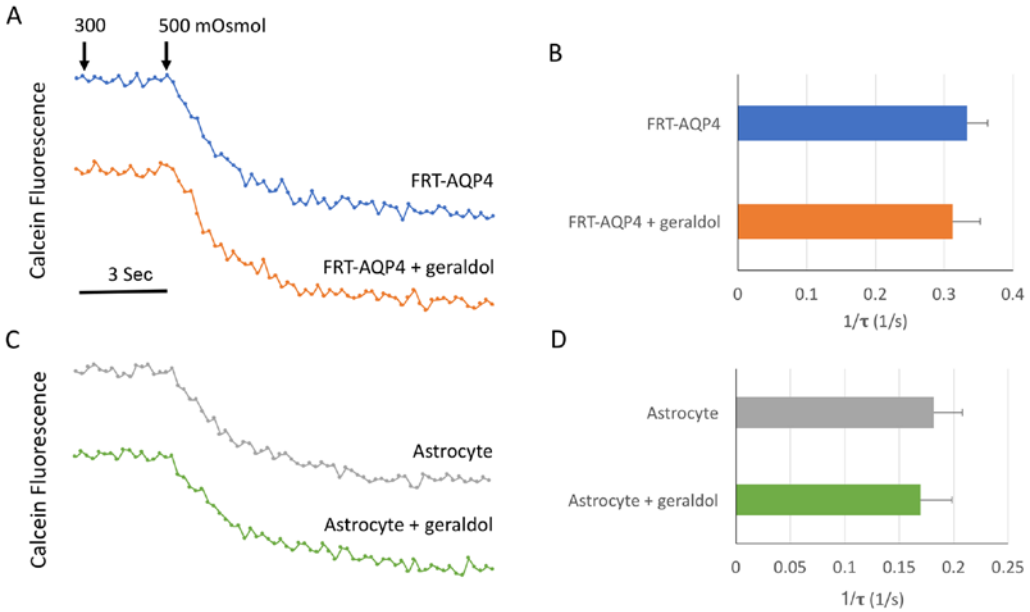

Figure 6. Effect of geraldol on water permeability in FRTL-AQP4 cells and primary astrocytes. (A) Representative curves of cell water permeability, presenting the time-course of calein fluorescence in response to changes in perfusate osmolality from 300-500 mOsmol in FRTL-AQP4 cells. (B) Cell shrinkage rates in FRTL-AQP4 cells assessed via reciprocal exponential time constants (1/sec). (C) Representative curves of cell water permeability showing the time-course of calcein fluorescence in response to changes in perfusate osmolality from 300 to 500 mOsmol in astrocytes. (D) Cell shrinkage rates in astrocytes assessed via reciprocal exponential time constants (1/sec) (n=6). AQP4, aquaporin 4.

Discussion

Serum NMO-IgG targets astrocytic AQP4, which is the most highly expressed aquaporin in astrocytes (6,35-37). NMO-IgG/AQP4 antibodies are present in up to 80% of patients with NMO (6,38-40). Although drugs and therapies are available for NMO, including methylprednisolone, immunosuppression and plasma exchange,

relapse may still occur, making NMO an incurable disease (9-11).

Inhibitors of NMO-IgG binding to AQP4 are potential therapeutic candidates for NMO. An ideal inhibitor should effectively block binding of NMO-IgG to AQP4 without harming other cells. In a previous study, inhibitors of NMO-IgG binding to AQP4 were identified (30). The activity of isotetrandrine, an alkaloid compound purified from fractions of *Mahonia japonica*, was demonstrated using a CDC experiment. It was also demonstrated that isotetrandrine had low cytotoxicity and did not affect the water transport function of AQP4 (30). In the present study, the inhibitory effect of a flavonoid compound (geraldol, purified from a fraction of *P. crispum*) on NMO-IgG binding to AQP4 was examined.

P. crispum, commonly known as parsley, is a culinary herb that was originally found in the Mediterranean region, but now grown worldwide. Its main constituents include coumarins, furanocoumarins (bergapten and imperatori), ascorbic acid, carotenoids, flavonoids, apiole, various terpenoic compounds, phenyl propanoids, phthalides and tocopherol (41,42). *P. crispum* has been used in a number of different medicinal applications, acting as an antimicrobial, antianemic, anticoagulant, antihyperlipidemic, antihypertensive, diuretic, hypoglycemic, hypouricemic, antioxidative and estrogenic agent (43). Geraldol was purified from *P. crispum* fractions via HPLC and it was demonstrated that this molecule inhibited binding of NMO-IgG to AQP4.

Geraldol is a flavonoid. Flavonoid compounds have broad biological properties, including antioxidative, free-radical scavenging, as well as anti-inflammatory/infective effects (44). These compounds usually have low cytotoxicity, and thus, may be safe for potential therapeutic use. Geraldol has been reported to show mild inhibitive effects against the interaction of human papillomavirus-16-E6 with caspase-8 (45). In addition, geraldol is a 3'-methoxylated metabolite of the flavonoid fisetin, which has distinct antioxidant, anti-inflammatory and anti-angiogenic properties (46).

Geraldol blocked NMO-IgG binding to AQP4 in immunofluorescence assays and reduced cytotoxicity in NMO-IgG/complement-treated FRTL-AQP4 cells and primary astrocytes. Furthermore, it did not affect the viability of FRTL-AQP4 cells and primary astrocytes, or water permeability in either cell system. These data suggest that geraldol is an effective inhibitor of NMO-IgG binding to AQP4, and could be a candidate molecule for use in NMO therapy.

Acknowledgements

Not applicable.

Funding

The present study was supported by he National Natural Science Fund (grant no. 81771304), the National Natural Science Youth Fund (grant no. 81601234 and 81601073), the Health Special Fund of Jilin Province (grant no. SCZSY201616), Science Technology Innovation Development Fund of Jilin (grant no. 201750246), Traditional Chinese Medicine Science and Technology Fund of Jilin Province (grant no. 2019140) and Jilin Province Health Research Talent Special Project Fund (grant no.2019SCZ037).

Availability of data and materials

The datasets used and/or analyzed during the current study are available from the corresponding author on reasonable request.

Authors' contributions

ML and MS designed the experiments and analyzed the experimental results. JW and SW carried out the experiments and wrote the manuscript. HX, WL, DW, LZ YL, JC and FL also performed the experiments, and helped write and review the manuscript. All authors read and approved the final manuscript.

Ethics approval and consent to participate

Protocols for mouse experiments were approved by The Laboratory Animal Ethics Committee of School of Life Science, Jilin University (Changchun, China; approval no. 2017-nsfc049). The use of patient blood samples was approved by Ethics Committee of The China-Japan Union Hospital, Jilin University (approval no. 2017022238). Written informed consent was obtained from all patients.

Patient consent for publication

Not applicable.

Competing interests

The authors declare that they have no competing interests.

References

1. Cree BA, Goodin DS and Hauser SL: Neuromyelitis optica. Semin Neurol 22: 105-122, 2002.
2. De Seze J, Lebrun C, Stojkovic T, Ferriby D, Chatel M and Vermersch P: Is Devic's neuromyelitis optica a separate disease? A comparative study with multiple sclerosis. Mult Scler 9: 521-525, 2003.
3. Hinson SR, Pittock SJ, Lucchinetti CF, Roemer SF, Fryer JP, Kryzer TJ and Lennon VA: Pathogenic potential of IgG binding to water channel extracellular domain in neuromyelitis optica. Neurology 69: 2221-2231, 2007.
4. Marignier R, Nicolle A, Watrin C, Touret M, Cavagna S, Varrin-Doyer M, Cavillon G, Rogemond V, Confavreux C, Honnorat J and Giraudon P: Oligodendrocytes are damaged by neuromyelitis optica immunoglobulin G via astrocyte injury. Brain 133: 2578-2591, 2010.
5. Parratt JD and Prineas JW: Neuromyelitis optica: A demyelinating disease characterized by acute destruction an regeneration of perivascular astrocytes. Mult Scler 16: 1156-1172, 2010.
6. Paul F, Jarius S, Aktas O, Bluthner M, Bauer O, Appelhans H, Franciotta D, Bergamaschi R, Littleton E, Palace J, *et al*: Antibody to aquaporin 4 in the diagnosis of neuromyelitis optica. PLoS Med 4: e133, 2007.
7. Matsuoka T, Matsushita T, Kawano Y, Osoegawa M, Ochi H, Ishizu T, Minohara M, Kikuchi H, Mihara F, Ohyagi Y and Kira J: Heterogeneity of aquaporin-4 autoimmunity and spinal cord lesions in multiple sclerosis in Japanese. Brain 130: 1206-1223, 2007.
8. Nicchia GP, Mastrototaro M, Rossi A, Pisani F, Tortorella C, Ruggieri M, Lia A, Trojano M, Frigeri A and Svelto M: Aquaporin-4 orthogonal arrays of particles are the target for neuromyelitis optica autoantibodies. Glia 57: 1363-1373, 2009.
9. Trebst C, Berthele A, Jarius S, Trebst C, Berthele A, Jarius S, Kümpfel T, Schippling S, Wildemann B and Wilke C; Neuromyelitis optica Studiengruppe (NEMOS): Diagnosis and treatment of neuromyelitis optica. Consensus recommendations of the neuromyelitis optica study group. Nervenarzt 82: 768-777, 2011 (In German).

10. Wildemann B, Jarius S and Paul F: Neuromyelitis optica. Nervenarzt 84: 436-441, 2013 (In German).
11. Kimbrough DJ, Fujihara K, Jacob A, Lana-Peixoto MA, Leite MI, Levy M, Marignier R, Nakashima I, Palace J, de Seze J, *et al*: Treatment of neuromyelitis optica: Review and recommendations. Mult Scler Relat Disord 1: 180-187, 2012.
12. Jarius S, Aboul-Enein F, Waters P, Kuenz B, Hauser A, Berger T, Lang W, Reindl M, Vincent A and Kristoferitsch W: Antibody to aquaporin-4 in the long-term course of neuromyelitis optica. Brain 131: 3072-3080, 2008.
13. Bedi GS, Brown AD, Delgado SR, Usmani N, Lam BL and Sheremata WA: Impact of rituximab on relapse rate and disability in neuromyelitis optica. Mult Scler 17: 1225-1230, 2011.
14. Kim SH, Kim W, Li XF, Jung IJ and Kim HJ: Repeated treatment with rituximab based on the assessment of peripheral circulating memory B cells in patients with relapsing neuromyelitis optica over 2 years. Arch Neurol 68: 1412-1420, 2011.
15. Greenberg BM, Graves D, Remington G, Hardeman P, Mann M, Karandikar N, Stuve O, Monson N and Frohman E: Rituximab dosing and monitoring strategies in neuromyelitis optica patients: Creating strategies for therapeutic success. Mult Scler 18: 1022-1026, 2012.
16. Pellkofer H, Suessmair C, Schulze A, Hohlfeld R and Kuempfel T: Course of neuromyelitis optica during inadvertent pregnancy in a patient treated with rituximab. Mult Scler 15: 1006-1008, 2009.
17. Costanzi C, Matiello M, Lucchinetti CF, Weinshenker BG, Pittock SJ, Mandrekar J, Thapa P and McKeon A: Azathioprine: Tolerability, efficacy, and predictors of benefit in neuromyelitis optica. Neurology 77: 659-666, 2011.
18. Watanabe S, Misu T, Miyazawa I, Nakashima I, Shiga Y, Fujihara K and Itoyama Y: Low-dose corticosteroids reduce relapses in neuromyelitis optica: A retrospective analysis. Mult Scler 13: 968-974, 2007.
19. Bichuetti DB, Lobato de Oliveira EM, Oliveira DM, Amorin de Souza N and Gabbai AA: Neuromyelitis optica treatment: Analysis of 36 patients. Mult Scler 67: 1131-1136, 2010.
20. Mandler RN, Ahmed W and Dencoff JE: Devic's neuromyelitis optica: A prospective study of seven patients treated with prednisone and azathioprine. Neurology 51: 1219-1220, 1998.
21. Jacob A, Matiello M, Weinshenker BG, Wingerchuk DM, Lucchinetti C, Shuster E, Carter J, Keegan BM, Kantarci OH and Pittock SJ: Treatment of neuromyelitis optica with mycophenolate mofetil: Retrospective analysis of 24 patients. Arch Neurol 66: 1128-1133, 2009.
22. Kitley J, Elsone L, George J, Waters P, Woodhall M, Vincent A, Jacob A, Leite MI and Palace J: Methotrexate is an alternative to azathioprine in neuromyelitis optica spectrum disorders with aquaporin-4 antibodies. J Neurol Neurosurg Psychiatry 84: 918-921, 2013.
23. Kim SH, Kim W, Park MS, Sohn EH, Li XF and Kim HJ: Efficacy and safety of mitoxantrone in patients with highly relapsing neuromyelitis optica. Arch Neurol 68: 473-479, 2011.
24. Weinstock-Guttman B, Ramanathan M, Lincoff N, Napoli SQ, Sharma J, Feichter J and Bakshi R: Study of mitoxantrone for the treatment of recurrent neuromyelitis optica (Devic disease). Arch Neurol 63: 957-963, 2006.
25. Cabre P, Olindo S, Marignier R, Jeannin S, Merle H and Smadja D; Aegis of French National Observatory of Multiple Sclerosis: Efficacy of mitoxantrone in neuromyelitis optica spectrum: Clinical and neuroradiological study. J Neurol Neurosurg Psychiatry 84: 511-516, 2013.
26. Dörr J, Bitsch A, Schmailzl KJ, Chan A, von Ahsen N, Hummel M, Varon R, Lill CM, Vogel HP, Zipp F and Paul F: Severe cardiac failure in a patient with multiple sclerosis following low-dose mitoxantrone treatment. Neurology 73: 991-993, 2009.
27. Stroet A, Hemmelmann C, Starck M, Zettl U, Dörr J, Friedemann P, Flachenecker P, Fleischer V, Zipp F, Nückel H, *et al*: Incidence of therapy-related acute leukaemia in mitoxantrone-treated multiple sclerosis patients in Germany. Ther Adv Neurol Disord 5: 75-79, 2012.
28. Stroet A, Gold R and Chan A: Acute myeloid leukemia in Italian patients with multiple sclerosis treated with mitoxantrone. Neurology 78: 933; author reply 933-934, 2012.
29. Tradtrantip L, Zhang H, Saadoun S, Phuan PW, Lam C, Papadopoulos MC, Bennett JL and Verkman AS: Anti-aquaporin-4 monoclonal antibody blocker therapy for neuromyelitis optica. Ann Neurol 71: 314-322, 2012.
30. Sun M, Wang J, Zhou Y, Wang Z, Jiang Y and Li M: Isotetrandrine reduces astrocyte cytotoxicity in neuromyelitis optica by blocking the binding of NMO-IgG to aquaporin 4. Neuroimmunomodulation 23: 98-108, 2016.
31. Solenov E, Watanabe H, Manley GT and Verkman AS: Sevenfold-reduced osmotic water permeability in primary astrocyte cultures from AQP-4-deficient mice, measured by a fluorescence quenching method. Am J Physiol Cell Physiol 286: C426-C432, 2004.
32. Li M, Su W, Wang J, Pisani F, Frigeri A and Ma T: Detection of anti-aquaporin-4 autoantibodies in the sera of Chinese neuromyelitis optica patients. Neural Regen Res 8: 708-713, 2013.
33. Khan M, Yu B, Rasul A, Al Shawi A, Yi F, Yang H and Ma T: Jaceosidin induces apoptosis in U87 glioblastoma cells through G2/M phase arrest. Evid Based Complement Alternat Med 2012: 703034, 2012.
34. Swanson RA, Liu J, Miller JW, Rothstein JD, Farrell K, Stein BA and Longuemare MC: Neuronal regulation of glutamate transporter subtype expression in astrocytes. J Neurosci 17: 932-940, 1997.
35. Lennon VA, Kryzer TJ, Pittock SJ, Verkman AS and Hinson SR: IgG marker of optic-spinal multiple sclerosis binds to the aquaporin-4 water channel. J Exp Med 202: 473-477, 2005.
36. Lennon VA, Wingerchuk DM, Kryzer TJ, Pittock SJ, Lucchinetti CF, Fujihara K, Nakashima I and Weinshenker BG: A serum autoantibody marker of neuromyelitis optica: Distinction from multiple sclerosis. Lancet 364: 2106-2112, 2004.
37. Jarius S, Franciotta D, Bergamaschi R, Wright H, Littleton E, Palace J, Hohlfeld R and Vincent A: NMO-IgG in the diagnosis of neuromyelitis optica. Neurology 68: 1076-1077, 2007.
38. Jarius S, Probst C, Borowski K, Franciotta D, Wildemann B, Stoecker W and Wandinger KP: Standardized method for the detection of antibodies to aquaporin-4 based on a highly sensitive immunofluorescence assay employing recombinant target antigen. J Neurol Sci 291: 52-56, 2010.
39. Jarius S, Franciotta D, Paul F, Bergamaschi R, Rommer PS, Ruprecht K, Ringelstein M, Aktas O, Kristoferitsch W and Wildemann B: Testing for antibodies to human aquaporin-4 by ELISA: Sensitivity, specificity, and direct comparison with immunohistochemistry. J Neurol Sci 320: 32-37, 2012.
40. Waters P, Jarius S, Littleton E, Leite MI, Jacob S, Gray B, Geraldes R, Vale T, Jacob A, Palace J, *et al*: Aquaporin-4 antibodies in neuromyelitis optica and longitudinally extensive transverse myelitis. Arch Neurol 65: 913-919, 2008.
41. Snoussi M, Dehmani A, Noumi E, Flamini G and Papetti A: Chemical composition and antibiofilm activity of *Petroselinum crispum* and *Ocimum basilicum* essential oils against Vibrio spp. strains. Microb Pathog 90: 13-21, 2016.
42. Chaudhary SK, Ceska O, Têtu C, Warrington PJ, Ashwood-Smith MJ and Poulton GA: Oxypeucedanin, a major furocoumarin in parsley, *Petroselinum crispum*. Planta Med 52: 462-464, 1986.
43. Mahmood S, Hussain S and Malik F: Critique of medicinal conspicuousness of parsley (*Petroselinum crispum*): A culinary herb of mediterranean region. Pak J Pharm Sci 27: 193-202, 2014.
44. Seelinger G, Merfort I and Schempp CM: Anti-oxidant, anti-inflammatory and anti-allergic activities of luteolin. Planta Med 74: 1667-1677, 2008.
45. Yuan CH, Filippova M, Tungteakkhun SS, Duerksen-Hughes PJ and Krstenansky JL: Small molecule inhibitors of the HPV16-E6 interaction with caspase 8. Bioorg Med Chem Lett 22: 2125-2129, 2012.
46. Jo JH, Jo JJ, Lee JM and Lee S: Identification of absolute conversion to geraldol from fisetin and pharmacokinetics in mouse. J Chromatogr B Analyt Technol Biomed Life Sci 1038: 95-100, 2016.